

ORIGINAL RESEARCH

The Effect of Metformin on Triple-Negative Breast Cancer Cells and Nude Mice

Jin Song, MD; Junfeng Du, Mmed; Lili Han, Mmed; Xue Lin, Bmed; Cibo Fan, Mmed; Gang Chen, Mmed

ABSTRACT

Triple-negative breast cancer (TNBC) presents the most adverse prognosis due to its pronounced invasive and metastatic features. Existing research has highlighted that metformin, a prevalent diabetes medication, possesses strong anti-tumor properties, particularly in inhibiting tumor invasion and metastasis. This study delves deeper into the impact of metformin on TNBC by examining changes in proliferation, apoptosis, invasion, migration, and adhesion of TNBC cells, specifically MDA-MB-231, post-metformin exposure. The treatment of MDA-MB-231 with metformin in immunodeficient nude mice led to discernible changes in tumor metrics such as size, weight, lymph node engagement, and angiogenesis. Post-treatment, MDA-MB-231 cells exhibited a marked decline in proliferation, invasion, migration, and adhesion, alongside

a significant rise in apoptosis. In the in vivo model with nude mice, tumors displayed notable reductions in size and weight post-metformin exposure. Furthermore, there was a pronounced decline in lymph node plasma cell proliferation and tumor angiogenesis. Through the use of both Enzyme-Linked Immunosorbent Assay and Real-Time Fluorescence Quantification, it was ascertained that the expression of Signal Transducer and Activator of Transcription 3 (STAT3) saw significant augmentation, while expressions of Matrix Metalloproteinase-2 (MMP-2), Matrix Metalloproteinase-9 (MMP-9), Interleukin-6 (IL-6), and Interleukin-7 (IL-7) decreased markedly. This suggests metformin's potential efficacy against TNBC, potentially mediated via the STAT3 signaling pathway and interleukins 6 and 7. (*Altern Ther Health Med.* 2023;29(8):389-395).

Jin Song, MD; Junfeng Du, Mmed; Lili Han, Mmed; Xue Lin, Bmed; Cibo Fan, Mmed; Gang Chen, Mmed; Department of general surgery, The Seventh Medical Center of Chinese PLA General Hospital, Beijing, China.

Corresponding author: Gang Chen, Mmed
E-mail: chengang0118@126.com

INTRODUCTION

Triple-negative breast cancer (TNBC) is distinguished by the absence of estrogen receptors (ER), progesterone receptors (PR), and human epidermal growth factor receptor 2 (HER2). It is predominantly diagnosed in premenopausal women and is known for its aggressive behavior. Patients diagnosed with TNBC have a five-year survival rate of less than 80%.¹ Characterized by rapid cell proliferation and pronounced tumor invasiveness, TNBC frequently metastasizes to internal organs, including the brain. The complexity of histopathological grading for such aggressive cancers has grown as oncology progresses.² In recent years, biomarkers such as ER, PR, and HER2 have been employed both as targets and prognostic indicators in TNBC treatment,³ paving the way for targeted

therapy. Nonetheless, the efficacy of common chemotherapy agents like cisplatin and carboplatin remains suboptimal for TNBC treatment. Consequently, surgery is often complemented with chemotherapy to enhance therapeutic outcomes.⁴

Tumor emergence often aligns with the initiation and progression of inflammation. In this context, elevated expression levels of interleukins IL-6 and IL-7 serve as potential early indicators of tumor onset.⁵ Matrix metalloproteinase (MMP), a calcium-dependent endopeptidase containing zinc, is pivotal in breaking down extracellular matrix proteins and is essential in tumor invasion and metastasis. It also plays roles in cell processes such as proliferation, apoptosis, migration, adhesion, and angiogenesis.⁶

Among matrix metalloproteinases, MMP-2 and MMP-9 have received considerable attention. MMP-2, targeting non-matrix proteins, supports vasoconstriction against tumors,⁷ whereas MMP-9 focuses on degrading and remodeling the extracellular matrix, activating other MMPs, and facilitating tumor cell infiltration.⁸ The Janus kinase/Signal transducer and activator of transcription 3 (JAK/STAT3) pathway is a cornerstone in tumor development. Aberrant expression of STAT3 in tumor tissues has been linked to tumor genesis and progression.⁹

Metformin, the primary therapeutic for type 2 diabetes,¹⁰ is water-soluble, but its oral absorption is subpar. In animal studies, it's typically delivered via intraperitoneal injection.¹¹ Emerging research has illuminated metformin's potential benefits, encompassing areas from treating polycystic ovary syndrome to offering cardiovascular protection and anti-tumor effects.¹² Notably, metformin has shown potential in activating MMP-2 and MMP-9, thereby inhibiting the invasion and metastasis of esophageal squamous cells.¹³ Its efficacy against TNBC, specifically through the activation of MMP-2 and MMP-9, is yet to be ascertained.

The MDA-MB-231 cell line, originating from the pleural fluid of a breast cancer patient, is a standard model in animal research.¹⁴ When inoculated into immunodeficient nude mice, these cells induce tumor formation, enabling in-depth study into the nuances of TNBC progression.¹⁵

This research delved into the impacts and mechanisms of metformin on TNBC, with an emphasis on assessing the expression of MMP-2, MMP-9, and STAT3 following metformin intraperitoneal injection in nude mice.

MATERIALS AND METHODS

Medicinal materials

The human triple-negative breast cancer cell line, MDA-MB-231, was obtained from the Cell Bank of the Chinese Academy of Sciences, Shanghai, China. Fetal bovine serum was sourced from Hangzhou Sijiqing Biological Engineering Technology Co., Ltd., Hangzhou, China. Dulbecco's Modified Eagle Medium (DMEM) came from Gibco, a Thermo Fisher Scientific subsidiary, Waltham, MA, USA. Sigma-Aldrich, St. Louis, MO, USA, provided trypsin, 3-(4,5-dimethylthiazol-2-yl)-2,5-diphenyltetrazolium bromide (MTT), and phosphate-buffered saline (PBS). Both cisplatin and metformin were acquired from Aladdin Industrial Corporation, Shanghai, China. Matrigel Matrix was secured from BD Biosciences, San Jose, CA, USA, while the Transwell Invasion Chamber came from Corning Costar, Corning, NY, USA. The BALB/c-nu nude mice were procured from Charles River Laboratories, Beijing, China.

All animal experiments adhered to the guidelines for the care and use of laboratory animals. They received approval from the institutional animal care and use committee at The Seventh Medical Center of Chinese PLA General Hospital (ly2021-0357).

Cell culture

MDA-MB-231 cells were cultivated in DMEM enriched with 10% fetal bovine serum, penicillin (100 U/mL), and streptomycin (100 µg/mL). These cell cultures thrived at a consistent 37°C with 5% CO₂ atmosphere. The growth of cells was diligently observed. Sub-culturing was executed when the confluency was between 70% and 80%, consistent with previously described procedures.¹⁶

Metformin IC50 test

The IC50 value for metformin was gauged using MDA-MB-231 cells. These cells were organized into seven groups:

control, positive control (6 mM cisplatin), and other specific experimental sets. This assessment adhered to a well-defined protocol,¹⁷ and the cell inhibition rate was computed based on the same.

Experimental grouping and administration

For subsequent experiments, MDA-MB-231 cells were categorized into three groups: blank control, positive control (6 mM cisplatin), and a metformin set (14 mM). Cell cultures were nurtured until they achieved roughly 50% confluence prior to further tests.

MTT colorimetric detection of cell proliferation

Cell proliferation rates were evaluated using the MTT assay, according to a previously defined protocol.¹⁸ Triple-negative breast cancer cells from the control, positive control, and metformin batches were allocated to a 96-well plate, maintaining a density of 8×10⁶ cells/L. The absorbance for each well was gauged using an enzyme-linked immunoassay, recording an absorbance of 490 nm. Subsequently, the cell inhibition rate was deduced.

Flow Cytometry Assessment of Cell Apoptosis

Flow cytometry was employed to quantify cell apoptosis across all groups, adhering to the apoptosis kit's guidelines as previously detailed.¹⁹ The apoptosis index (AI) was derived using the formula: AI = number of apoptotic cells/(number of apoptotic cells + normal cells).

Transwell Assay for Cell Invasion Evaluation

The Transwell assay facilitated the assessment of cell invasion. Triple-negative breast cancer cells from each group were standardized to a concentration of 1 × 10⁴ cells/mL, with the procedure following established protocols.¹⁸ Invaded cells were tallied across ten arbitrary microscope fields, and the average value was documented as the definitive invasion count.

Scratch Assay for Cell Migration

Migration potential of MDA-MB-231 cells was gauged using the scratch assay in line with prior protocols.²⁰ Cells, once seeded onto a 24-well plate and achieving 70% confluence, underwent serum deprivation in DMEM for 24 hours. A sterilized pipette tip created a scratch, post which the cells were cleansed and monitored over a 24-hour period for migratory behavior.

Stromal Adhesion Test for Cell Adherence

A stromal adhesion assay was used to appraise cell adhesion. Matrigel, when diluted in serum-free DMEM, was coated onto a 96-well plate and air-dried for the night. Cells, after exposure to IC50 metformin concentrations, were seeded and kept under conditions of 37°C and 5% CO₂ for a span of 2 hours. MTT was subsequently added, and the relative adhesion rate was deduced, as laid out in prior procedures.¹⁸

Tumor Inoculation in Nude Mice

Experiments involving tumor inoculation were executed with 5-week-old BALB/c-nu nude mice situated in an SPF environment. MDA-MB-231 cells of the triple-negative breast cancer variety were injected into the mice. This was followed by a cyclophosphamide dosage. Tumor progression was charted over a fortnight. Once the drug was administered, the mice were euthanized at varying intervals, recording tumor dimensions and mass as previously noted.²¹

Immunohistochemical Analysis

Lymphatic tissues from mice post metformin intervention were analyzed using immunohistochemistry as outlined in prior protocols.²² After processing the tissues, they underwent antibody staining with Anti-CD20 and Anti-CD3 Gamma primary antibodies, complemented by PV-9001 reagent secondary antibodies. Hematoxylin staining enabled visualization of the results.

Evaluation of Tumor Vascular Structure and Treatment Impact

The influence of metformin on the tumor's vascular network was examined employing the Endra Nexus 128 photoacoustic imaging system, adhering to previously documented methods.²³ After the induction of anesthesia, a tail vein injection of Gold nanostar was administered. Osirix software facilitated a three-dimensional visualization of the tumor structures.

Enzyme-linked immunosorbent assay (ELISA)

For the quantification of specific proteins, ELISA was executed on pancreatic tissue homogenates derived from the nude mice, following established protocols.²⁴

Real-Time Polymerase Chain Reaction (RT-PCR) Analysis

The relative expression levels of genes MMP-2, MMP-9, and STAT3 within the tumor samples were quantified using real-time fluorescence quantification polymerase chain reaction (RT-PCR), as delineated in prior research.²⁵ The specific primers utilized are enumerated in Table 11.

Statistical Methods

Every experiment was executed in a triplicate format. Except for specific mentions, all data representation follows the format Mean ± SEM. GraphPad Prism 8.0 (GraphPad Software, San Diego, CA, USA) facilitated data management and histogram creation. Statistical computations,

Table 1. Metformin IC50 curve.

Item	Control	Control-positive	Metformin groups (mM)				
			5	10	15	20	30
OD _{490nm}	0.979	0.29 ± 0.01	0.72 ± 0.01	0.60 ± 0.01	0.43 ± 0.01	0.31 ± 0.01	0.12 ± 0.01
Inhibition rate (%)	/	70.9 ± 0.18	26.3 ± 0.258	38.7 ± 0.27	56.5 ± 0.09	68.4 ± 0.12	87.7 ± 0.09

Table 2. The effects of metformin on the proliferation and apoptosis of MDA-MB-231 cells.

Group	Inhibition rate (%)	P value	Apoptosis rate (%)	P value
Control	1.17 ± 0.04	/	0.93 ± 0.03	/
Control-positive	52.5 ± 0.24	<.0001	15.7 ± 0.11	<.0001
Metformin	48.9 ± 0.17	<.0001	11.3 ± 0.02	<.0001

Table 3. The influence of metformin on the invasion and migration of MDA-MB-231 cells.

Group	Invasive cell number	P value	Migration ability (%)	P value
Control	133 ± 0.93	<.0001	100 ± 0.00	/
Control-positive	35.4 ± 1.16	<.0001	22.1 ± 0.19	<.0001
Metformin	43.3 ± 1.04	<.0001	39.6 ± 0.32	<.0001

Table 4. The influence of metformin on the adhesion ability of MDA-MB-231 cells.

Group	OD value	Adhesion rate (%)	P value
Control	1.71 ± 0.01	100 ± 0.00	/
Control-positive	0.49 ± 0.01	28.7 ± 0.60	<.0001
Metformin	0.64 ± 0.03	37.5 ± 1.82	<.0001

Table 5. Tumor growth curve.

Item	Time (day)							
	0	2	4	6	8	10	12	14
tumor volume (3 mm)	0.00 ± 0.00	28.5 ± 1.39	69.4 ± 1.35	147 ± 1.77	266 ± 2.38	362 ± 2.44	505 ± 3.27	636 ± 4.28
P value	/	<.0001	<.0001	<.0001	<.0001	<.0001	<.0001	<.0001

Table 6. The effect of metformin on tumor size (volume).

Group	Time (day) tumor volume (3 mm)								n
	0	1	2	3	4	5	6	7	
Control	637 ± 2.30	686 ± 2.90	712 ± 1.58	755 ± 3.22	808 ± 2.60	845 ± 2.33	887 ± 3.28	923 ± 2.85	10
Control-positive	638 ± 0.78	572 ± 2.03	520 ± 0.88	472 ± 3.46	433 ± 1.20	373 ± 2.91	299 ± 1.73	248 ± 1.16	10
Metformin	640 ± 0.32	592 ± 1.73	581 ± 1.53	561 ± 1.16	517 ± 2.08	476 ± 2.08	421 ± 1.16	384 ± 1.73	10

Table 7. The effect of metformin on tumor weight.

Group	Time (day) tumor weight (g)								n
	0	1	2	3	4	5	6	7	
Control	0.68 ± 0.01	0.72 ± 0.02	0.77 ± 0.01	0.84 ± 0.01	0.89 ± 0.01	0.94 ± 0.01	0.98 ± 0.01	1.05 ± 0.01	10
Control-positive	0.76 ± 0.02	0.68 ± 0.02	0.63 ± 0.01	0.56 ± 0.01	0.49 ± 0.01	0.42 ± 0.01	0.34 ± 0.01	0.25 ± 0.02	10
Metformin	0.71 ± 0.01	0.67 ± 0.01	0.63 ± 0.01	0.58 ± 0.01	0.54 ± 0.01	0.49 ± 0.01	0.44 ± 0.01	0.39 ± 0.01	10

Table 8. The effect of metformin on tumor blood vessels.

Group	Time (h) normalized signal						n
	0	2	4	6	12	24	
Control	0.95 ± 0.02	2.64 ± 0.31	4.61 ± 0.22	6.67 ± 0.20	5.83 ± 0.23	5.01 ± 0.19	10
Control-positive	0.99 ± 0.01	1.56 ± 0.03	2.29 ± 0.05	1.97 ± 0.03	1.56 ± 0.04	1.30 ± 0.01	10
Metformin	1.00 ± 0.01	1.82 ± 0.02	3.4 ± 0.03	2.63 ± 0.03	2.07 ± 0.03	1.62 ± 0.04	10

Table 9. The expression of MMP-2, MMP-9, STAT3, IL-6 and IL-7 at the protein level.

Group	OD450				
	MMP-2	MMP-9	STAT3	IL-6	IL-7
Control	3.24 ± 0.01	4.07 ± 0.01	1.21 ± 0.01	2.38 ± 0.02	2.70 ± 0.01
Control-positive	1.31 ± 0.01	1.44 ± 0.02	4.58 ± 0.02	0.46 ± 0.02	0.34 ± 0.02
Metformin	1.70 ± 0.01	1.98 ± 0.02	3.22 ± 0.02	0.94 ± 0.03	0.66 ± 0.01

Table 10. The expression of MMP-2, MMP-9, STAT3, IL-6 and IL-7 at the mRNA level.

Group	MMP-2	MMP-9	STAT3	IL-6	IL-7
Control	3.65 ± 0.02	4.31 ± 0.02	0.62 ± 0.02	4.22 ± 0.02	5.78 ± 0.06
Control-positive	0.36 ± 0.02	0.38 ± 0.01	3.85 ± 0.02	0.70 ± 0.02	0.43 ± 0.02
Metformin	1.35 ± 0.02	1.59 ± 0.02	3.09 ± 0.02	0.97 ± 0.03	1.19 ± 0.03

Table 11. Primer sequence.

Primer sequence	Forward Primer	Reverse Primer
MMP-2	5'-GGATGATGCCnll'GCTCG-3'	5'-CAGTGGACATGGCGGTCT-3'
MMP-9	5'-AACTCACGCGCCAGTAGAAG-3'	5'-GAGGTGGACCGGATGTTCC-3'
IL-6	5'-CTGCAAGAGACTTCCATCCAG-3'	5'-AGTGTATAGACAGGTCTGTGG-3'
IL-7	5'-TTCCTCCACTGATCCTTGTCT-3'	5'-AGCAGCTTCCTTTGTATCATCAC-3'
STAT3	5'-CACCTTGGATTGAGAGTCAAGAC-3'	5'-AGGAATCGGCTATATTGCTGGT-3'
β-actin	5'-ATCTGGCAC CACACCTTCAATGAGCTGCG-3'	5'-CGTCATCCCTGCTTGTGATCCA CATTCG-3'

Figure 1. The effect of metformin on MDA-MB-231 cells. **A.** Metformin structural formula; **B.** Metformin IC50 curve; **C.** Statistical graph of cell proliferation inhibition; **D.** Statistical graph of cell apoptosis; **E.** Flow cytometric graph of cell apoptosis

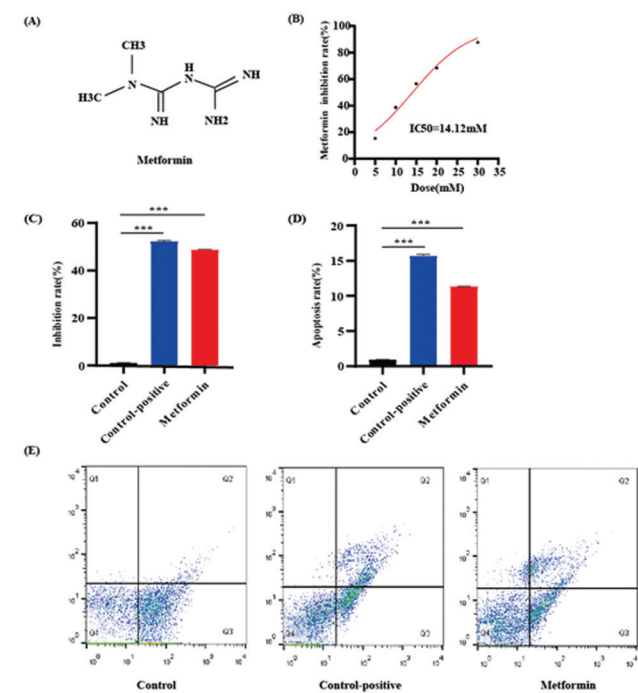
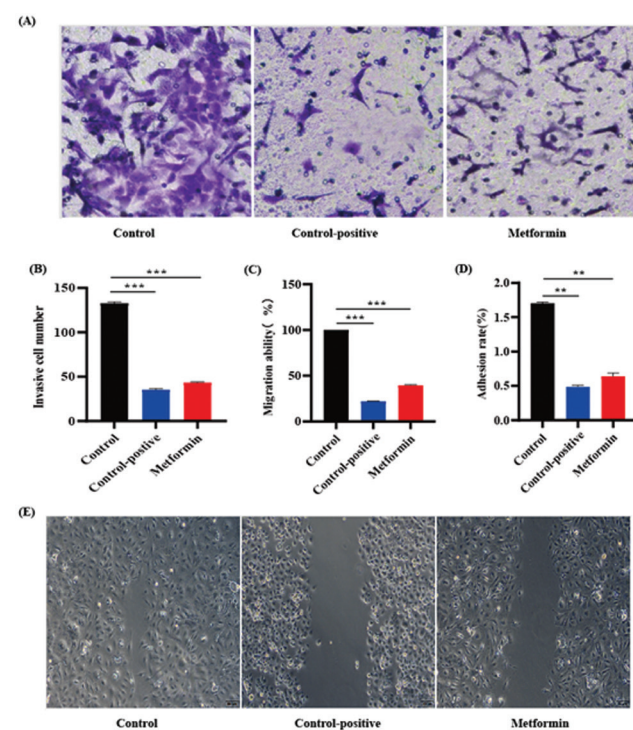


Figure 2. The effect of metformin on MDA-MB-231 cells. **A.** Effect graph of cell invasion; **B.** Statistical graph of cell invasion; **C.** Effect graph of cell migration; **D.** Detection of cell relative adhesion; **E.** Effect graph of cell scratch experiment



inclusive of the *t* test and rank-sum test, were executed using SPSS 26.0 (IBM Corp., Armonk, NY, USA). For all statistical outputs, a *P* < .05 was deemed as denoting significant difference.

RESULTS

Metformin's Influence on MDA-MB-231 Cells

Metformin, synthesized from the reaction between dimethylamine and dicyandiamide resulting in a salt, bears the molecular formula C₄H₁₁N₅ (Figure 1A). Our objective was to discern the optimal concentration of metformin for MDA-MB-231, a triple-negative breast cancer cell line. Testing was conducted with varying metformin concentrations (5 mM, 10 mM, 15 mM, 20 mM, and 30 mM), and we employed the MTT assay to gauge the cell inhibition rate for each group, plotting the results on the IC₅₀ curve (Figure 1B, Table 1). The IC₅₀ value of metformin was determined to be 14.12 mM.

Based on this IC₅₀ value, 14 mM was selected as the optimal dosage of metformin. Our study encompassed three groups: the control, the positive control (6 mM cisplatin), and the experimental (14 mM metformin). After administering the respective treatments to MDA-MB-231 cells, we investigated various cellular behaviors including proliferation, apoptosis, invasion, migration, and adhesion. Notably, both the positive control and experimental groups demonstrated a significant increase in the inhibition rate of cell proliferation and apoptosis when compared to the control group (Figure 1C-E, Table 2). Evaluating invasion and migration revealed that the abilities of MDA-MB-231 cells to invade and migrate were markedly diminished in the positive control and experimental groups compared to the control group (Figure 2A-C, 2E, Table 3). Adhesion assessment through a microplate reader underscored that the

relative adhesion rate of cells treated with the positive drug agents (cisplatin and metformin) was appreciably reduced relative to the control group (Figure 2D, Table 4).

Establishing the MDA-MB-231 Tumor Model in Nude Mice

The study employed BALB/c-nu nude mice as the animal model. After subcutaneously injecting MDA-MB-231 cell suspension into the axillary region of these mice, we diligently monitored them over a span of two weeks, recording tumor dimensions and drafting a tumor growth curve. The results unveiled consistent tumor growth in the aftermath of the MDA-MB-231 cell injection (Figure 3A, Table 5).

Effect of Metformin on Tumorigenesis in MDA-MB-231 Nude Mice

Upon successfully establishing the mouse model, we initiated treatment with metformin at a concentration of 22 mM. We subsequently assessed parameters like tumor dimensions, weight, lymphatic node development, and angiogenesis. The data illustrated a notable decrease in both tumor size (Figure 3B, Table 6) and weight (Figure 3C, Table 7) in the mice treated with either the positive control drug, cisplatin (20 mM), or metformin. Following seven days of treatment, the mice were euthanised, and lymphatic node samples were extracted and subjected to immunohistochemistry. This analysis revealed a significant diminishment in lymph node plasma cell proliferation in both the positive control and experimental groups, compared to the untreated controls. Interestingly, the positive control group displayed superior inhibitory effects (Figure 3D). The application of a sophisticated optical imaging system for 3D visualization of tumor vasculature further indicated substantial angiogenic suppression in both the positive control and metformin-treated mice when juxtaposed with the untreated control group (Figure 3E-F, Table 8).

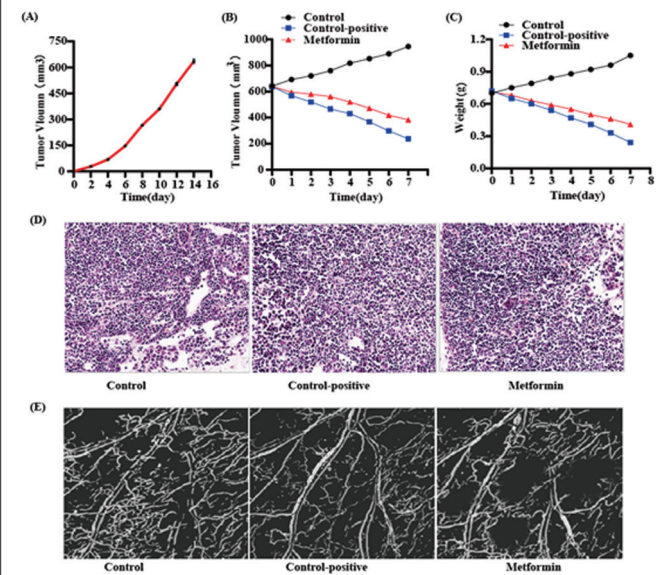
Metformin's Influence on Molecular Expressions in MDA-MB-231 Nude Mice

Delving into molecular mechanisms, our ELISA experiments uncovered intriguing findings post-metformin administration. Specifically, while STAT3 expression saw a marked increase in treated mice compared to controls, the expression patterns for MMP-2, MMP-9, IL-6, and IL-7 witnessed a significant decline (Figure 3G, Table 9). Amplifying these findings, real-time fluorescence quantification (RT-PCR) further corroborated the altered gene expression. The data elucidated an upregulated STAT3 mRNA expression in the treated mice, contrasted by pronounced downregulation in mRNA levels of MMP-2, MMP-9, IL-6, and IL-7 (Figure 3H, Table 10 and Table 11).

DISCUSSION

TNBC is particularly menacing among breast cancer subtypes due to its aggressive nature and lack of targeted therapies. Characterized by the absence of estrogen, progesterone, and HER2/neu receptors, TNBC is refractory

Figure 3. The effect of metformin on MDA-MB-231 nude mice. **A.** Tumor growth curve after modeling; **B.** The effect of metformin on tumor size; **C.** The effect of metformin on tumor weight; **D.** The effect of metformin on lymph nodes; **E.** The effect of metformin on tumor blood vessels; **F.** The effect of tumor blood vessels Analysis of photoacoustic signal intensity; **G.** Expression of MMP-2, MMP-9, STAT3, IL-6 and IL-7 at the protein level (**H**) MMP-2, MMP-9, STAT3, IL-6 and IL-7 Expression at the mRNA level



to hormone and targeted therapies that have shown efficacy in other breast cancer subtypes. As a consequence, patients with TNBC often face limited treatment options, relying predominantly on systemic chemotherapies that often come with high recurrence rates.³ This dearth of effective treatments for TNBC underscores the urgent need for alternative therapeutics. The demonstrated efficacy of platinum-based drugs like cisplatin, despite recurrence challenges, led us to utilize it as a comparative standard for metformin.²⁶

Metformin, traditionally an anti-diabetic, has recently been highlighted for its broader applications, including weight loss and anti-aging benefits. Its observed lifespan extension effects in *Caenorhabditis elegans* via gut microbiota modulation underscore its potential therapeutic versatility.²⁷ A compelling attribute is metformin's ability to inhibit tumor growth by activating AMP-activated protein kinase (AMPK), a central metabolic switch that regulates energy homeostasis. This effect poses a formidable countermeasure against tumor progression, positioning metformin as a promising oncological therapeutic.²⁸

Cisplatin was selected as the positive control in our study due to its established efficacy against a spectrum of solid tumors, including TNBC. As an alkylating agent, cisplatin introduces DNA cross-links that obstruct DNA replication, leading to cell cycle arrest and apoptosis. Its clinical effectiveness against TNBC provided a stringent benchmark against which the effects of metformin could be measured. Furthermore, its well-characterized mechanism of

action and pharmacodynamics offer a valuable comparator when deciphering metformin's potential anti-TNBC effects.

In the context of TNBC, the upregulated expression of MMP-2 and MMP-9 are hallmarks, playing crucial roles in tumor growth and metastasis.²⁹ Simultaneously, STAT3, a primary transcription activator, modulates MMP-2 expression, emphasizing the interconnectedness of these pathways. The aberrant levels of interleukins IL-6 and IL-7, which are disproportionately elevated in TNBC patients compared to non-TNBC individuals, further compound the disease's complexity.³⁰

Our comprehensive analysis aimed to elucidate metformin's therapeutic efficacy against TNBC using MDA-MB-231 cells as a model. In vitro findings highlighted metformin's potential in inhibiting cell proliferation and promoting apoptosis. Although cisplatin's efficacy was superior, metformin notably impeded cell invasion, migration, and adhesion.

The in vivo experiments provided compelling evidence of metformin's potential anti-tumor effects. Tumor-bearing nude mice treated with metformin exhibited significant reductions in tumor dimensions and weight. Further reinforcing these findings, the reduced plasma cell proliferation in lymph nodes and diminished tumor vasculature illuminated metformin's multi-faceted anti-tumor mechanisms. The anti-tumor properties of metformin are believed to be predominantly mediated through its activation of AMP-activated protein kinase (AMPK). This enzyme, central to cellular energy homeostasis, when activated by metformin, inhibits the mechanistic target of rapamycin (mTOR), a key promoter of cell growth and proliferation. The subsequent downregulation of mTOR suppresses protein synthesis and cell cycle progression, effectively stymying tumor growth.

Within the TNBC milieu, the matrix metalloproteinases MMP-2 and MMP-9 are known facilitators of tumor invasion and metastasis, contributing to the aggressive nature of this cancer subtype. Their activity is closely regulated by various signaling pathways, notably the STAT3 cascade. The STAT3 transcription activator, when aberrantly activated, drives the expression of numerous genes, including MMP-2, facilitating tumor progression. Metformin's observed downregulation of MMP-2 and MMP-9, along with its contrasting upregulation of STAT3, is a pivotal discovery. It suggests that metformin might be rewiring the molecular circuitry of TNBC, offering potential therapeutic leverage points. Taken together, the mechanistic insights gleaned from our study spotlight metformin as a multifaceted therapeutic candidate, capable of modulating both cellular metabolism and key signaling pathways integral to TNBC progression.

CONCLUSION

In sum, our investigation unveils metformin's potential as a TNBC therapeutic. Its capacity to impede the pathophysiological hallmarks of TNBC, including cell proliferation, migration, and invasion, alongside promoting

apoptosis and reducing adhesion, is notable. Importantly, in vivo studies further supported these findings, showcasing tumor size and weight reduction. At the molecular juncture, metformin's regulatory effects on the STAT3 signaling pathway, leading to modulated gene expression, offer a mechanistic insight. Collectively, these findings position metformin as a promising therapeutic candidate against TNBC, potentially mediated through the STAT3 signaling cascade and its downstream targets.

DATA AVAILABILITY

The original contributions presented in the study are included in the article/Supplementary Material. Further inquiries can be directed to the corresponding authors.

AUTHOR CONTRIBUTIONS

Jin Song conducted the cell-based experiments, analyzed the data, and contributed to the manuscript drafting. Junfeng Du executed the in vivo experiments on nude mice, assisted in data analysis and interpretation, and participated in drafting the manuscript. Lili Han engaged in molecular studies (ELISA and RT-PCR), data analysis, and manuscript preparation. Xue Lin carried out the cell invasion, migration, and adhesion assays, helped with data interpretation, and contributed to manuscript drafting. Cibo Fan helped determine the IC50 of metformin, and participated in data analysis, and manuscript drafting. Gang Chen, the corresponding author, conceptualized and led the project, supervised all the experiments, oversaw data analysis and interpretation, corresponded with the journal during submission and revision, and took responsibility for finalizing the manuscript. All authors have read and approved the final manuscript.

ACKNOWLEDGMENT

The authors would like to express their profound gratitude to all the Department of General Surgery staff at The Seventh Medical Center of Chinese PLA General Hospital for their invaluable assistance and support throughout this research. We also extend our sincere thanks to our families and colleagues for their understanding, encouragement, and technical advice during the course of the project. Furthermore, we are immensely grateful for the constructive criticism and suggestions provided by the anonymous reviewers, which significantly improved the quality of this manuscript.

ETHICAL STATEMENT

This study was carried out in strict accordance with the recommendations in the Guide for the Care and Use of Laboratory Animals of the National Institutes of Health. The experimental protocol was approved by the committee on the Ethics of Animal Experiments of the Seventh Medical Center of Chinese PLA General Hospital (ly2021-0357). All surgery was performed under sodium pentobarbital anesthesia, and every effort was made to minimize suffering. The principles of the 3Rs (Replacement, Reduction, and Refinement) were followed during all animal procedures. The study also adhered to the ethical guidelines for research involving human subjects, where applicable.

REFERENCE

- Zagami P, Carey LA. Triple negative breast cancer: pitfalls and progress. *NPJ Breast Cancer*. 2022;8(1):95. doi:10.1038/s41523-022-00468-0
- Derakhshan F, Reis-Filho JSJ. Pathogenesis of triple-negative breast cancer. *Annu Rev Pathol*. 2022;17(1):181-204. doi:10.1146/annurev-pathol-042420-093238
- Yin L, Duan JJ, Bian XW, Yu SC. Triple-negative breast cancer molecular subtyping and treatment progress. *Breast Cancer Res*. 2020;22(1):61. doi:10.1186/s13058-020-01296-5
- Lynce F, Nunes R. Role of Platinum in Triple-Negative Breast Cancer. *Curr Oncol Rep*. 2021;23(5):50. doi:10.1007/s11912-021-01041-x
- Knochemann HM, Dwyer CJ, Smith AS, et al. IL6 Fuels Durable Memory for Th17 Cell-Mediated Responses to Tumors. *Cancer Res*. 2020;80(18):3920-3932. doi:10.1158/0008-5472.CAN-19-3685
- Carriero S, Lanza C, Pellegrino G, et al. Ablative Therapies for Breast Cancer: state of Art. *Technol Cancer Res Treat*. 2023;22:15330338231157193. doi:10.1177/15330338231157193
- Machado BC, Gutierrez PT, Juliana M-R, et al. Ab'Saber Alexandre, Takagaki Teresa, Capelozzi Vera Luiza. Modeling extracellular matrix through histo-molecular gradient in NSCLC for clinical decisions. *Front Oncol*. 2022;12:1042766. doi:10.3389/fonc.2022.1042766
- Puttipanyalears C, Denariyakoon S, Angsuwatcharakon P, et al. Quantitative STAU2 measurement in lymphocytes for breast cancer risk assessment. *Sci Rep*. 2021;11(1):915. doi:10.1038/s41598-020-79622-2
- Sonnenblick A, Agbor-Tarh D, de Azambuja E, et al. STAT3 activation in HER2-positive breast cancers: analysis of data from a large prospective trial. *Int J Cancer*. 2021;148(6):1529-1535. doi:10.1002/ijc.33385
- Sonnenblick A, Agbor-Tarh D, de Azambuja E, et al. STAT3 activation in HER2-positive breast cancers: analysis of data from a large prospective trial. *Int J Cancer*. 2021;148(6):1529-1535. doi:10.1002/ijc.33385
- Choi SY, Lee C, Heo MJ, et al. Metformin ameliorates animal models of dermatitis. *Inflammopharmacology*. 2020;28(5):1293-1300. doi:10.1007/s10787-020-00704-8
- Karmanova E, Chernikov A, Usacheva A, Ivanov V, Bruskov V. Metformin counters oxidative stress and mitigates adverse effects of radiation exposure: an overview. *Fundam Clin Pharmacol*. 2023;37(4):713-725. doi:10.1111/fcp.12884
- Li WD, Li NP, Song DD, Rong JJ, Qian AM, Li XQ. Metformin inhibits endothelial progenitor cell migration by decreasing matrix metalloproteinases, MMP-2 and MMP-9, via the AMPK/mTOR/autophagy pathway. *Int J Mol Med*. 2017;39(5):1262-1268. doi:10.3892/ijmm.2017.2929
- Pan S, Zhao X, Shao C, et al. STIM1 promotes angiogenesis by reducing exosomal miR-145 in breast cancer MDA-MB-231 cells. *Cell Death Dis*. 2021;12(1):38. PMID:33414420 doi:10.1038/s41419-020-03304-0
- Tseng TH, Chien MH, Lin WL, et al. Inhibition of MDA-MB-231 breast cancer cell proliferation and tumor growth by apigenin through induction of G2/M arrest and histone H3 acetylation-mediated p21WAF1/CIP1 expression. *Environ Toxicol*. 2017;32(2):434-444. PMID:26872304 doi:10.1002/tox.22247
- Huang Z, Yu P, Tang J. Characterization of Triple-Negative Breast Cancer MDA-MB-231 Cell Spheroid Model. *OncoTargets Ther*. 2020;13:5395-5405. doi:10.2147/OTT.S249756

17. Azami H, Malek-Hosseini S, Mojahed Taghi M, Zareinejad M, Amirghofran Z. Antitumor Activity and Immunomodulatory Effects of *Ficus carica* Latex. *Journal of Shahid Sadoughi University of Medical Sciences*. 2021;28(12). doi:10.18502/ssu.v28i12.5776
18. Yang A, et al. *Effects of NRP2mAb on proliferation, migration, invasion and adhesion of breast cancer cells*. *Oncology Progress*; 2019.
19. Ren ZQ, Yan WJ, Zhang XZ, Zhang PB, Zhang C, Chen SK. CUL1 Knockdown Attenuates the Adhesion, Invasion, and Migration of Triple-Negative Breast Cancer Cells via Inhibition of Epithelial-Mesenchymal Transition. *Pathol Oncol Res*. 2020;26(2):1153-1163. doi:10.1007/s12253-019-00681-6
20. Wang W, Zhang R, Wang X, et al. Suppression of KIF3A inhibits triple negative breast cancer growth and metastasis by repressing Rb-E2F signaling and epithelial-mesenchymal transition. *Cancer Sci*. 2020;111(4):1422-1434. doi:10.1111/cas.14324
21. Dong J, Chen Y, Yang W, Zhang X, Li L. Antitumor and anti-angiogenic effects of artemisinin on breast tumor xenografts in nude mice. *Res Vet Sci*. 2020;129:66-69. doi:10.1016/j.rvsc.2020.01.005
22. Yeong J, Tan T, Chow ZL, et al. Multiplex immunohistochemistry/immunofluorescence (mIHC/IF) for PD-L1 testing in triple-negative breast cancer: a translational assay compared with conventional IHC. *J Clin Pathol*. 2020;73(9):557-562. PMID:31969377 doi:10.1136/jclinpath-2019-206252
23. Tezcan O, Elshafei AS, Benderski K, et al. Effect of Cellular and Microenvironmental Multidrug Resistance on Tumor-Targeted Drug Delivery in Triple-Negative Breast cancer. *J Control Release*. 2023;354:784-793. PMID:36599395 doi:10.1016/j.jconrel.2022.12.056
24. Golakiya A, Patel J, Haldar S. (2021). MTT assay on HL60 and Jurkat cell lines. *ELISA assay for the quantification of IgA in human serum*. doi:10.13140/RG.2.2.20577.22885.
25. Ramesh A, Deshpande N, Malik V, Nguyen A, Malhotra M, Debnath M, Brouillard A, Kulkarni A. (2023). Activatable Nanoreporters for Real-Time Tracking of Macrophage Phenotypic States Associated with Disease Progression. *Small* 2300978. <https://doi.org/10.1002/sml.202300978>
26. Bellon JR, Chen YH, Rees R, et al. A Phase 1 Dose-Escalation Trial of Radiation Therapy and Concurrent Cisplatin for Stage II and III Triple-Negative Breast Cancer. *Int J Radiat Oncol Biol Phys*. 2021;111(1):45-52. PMID:33713742 doi:10.1016/j.ijrobp.2021.03.002
27. Espada L, Dakhovnik A, Chaudhari P, et al. Loss of metabolic plasticity underlies metformin toxicity in aged *Caenorhabditis elegans*. *Nat Metab*. 2020;2(11):1316-1331. PMID:33139960 doi:10.1038/s42255-020-00307-1
28. Sasaki H, Asanuma H, Fujita M, et al. Metformin prevents progression of heart failure in dogs: role of AMP-activated protein kinase. *Circulation*. 2009;119(19):2568-2577. PMID:19414638 doi:10.1161/CIRCULATIONAHA.108.798561
29. Huang Q, Li S, Zhang L, et al. CAPE-pNO₂ Inhibited the Growth and Metastasis of Triple-Negative Breast Cancer via the EGFR/STAT3/Akt/E-Cadherin Signaling Pathway. *Front Oncol*. 2019;9:461. PMID:31214503 doi:10.3389/fonc.2019.00461
30. Das S, De S, Sengupta S. Post-transcriptional regulation of MMP2 mRNA by its interaction with miR-20a and Nucleolin in breast cancer cell lines. *Mol Biol Rep*. 2021;48(3):2315-2324. PMID:33788053 doi:10.1007/s11033-021-06261-9